

Scalar mixing in a free, turbulent rectangular jet

E. W. GRANDMAISON,† A. POLLARD‡ and S. NG†

† Department of Chemical Engineering, Queen's University, Kingston, Ontario,
Canada K7L 3N6

‡ Department of Mechanical Engineering, Queen's University, Kingston, Ontario, Canada K7L 3N6

(Received 28 June 1989 and in final form 29 August 1990)

Abstract—The scalar mixing field of a turbulent jet issuing from a sharp-edged rectangular orifice with an aspect ratio of 10 is investigated using marker nephelometry. Results include the mean and fluctuation concentration field of nozzle fluid and intermittency. In the near region of the flow, the mean concentration decay is characterized by the narrow dimension of the jet, the saddle-back profile characteristic of the velocity field is observed and good symmetry is demonstrated for the scalar properties. In the far field of the flow, the mean concentration decay is characterized by a length scale equivalent to a round jet with the same orifice area. Based on this length scale the centreline mean concentration decay is about twice that of a round jet. In addition the transverse profiles of the mean concentration, fluctuation concentration and intermittency exhibit a departure from symmetry in both planes.

INTRODUCTION

IN HEAT and mass transfer operations, turbulent jet flows have found wide application where dispersion of material is required. Examples are mixing limited gas phase reactions (combustion) and dispersion of material and energy sources in various chemical and environmental applications. A primary interest in these systems is the mixing and entrainment behaviour of turbulent jets with a surrounding fluid or selective mixing with another fluid stream involved in the process. Direct measurements of entrainment of the turbulent jet in free, stagnant surroundings have been made, for example, by Ricoh and Spalding [1]. Techniques for measuring the mixing between different jet streams have been demonstrated by Becker and Booth [2]. Information regarding the mixing field of a round free jet has also been obtained from measurements of the mean and fluctuation properties of the nozzle fluid [3]. The scalar concentration and intermittency data from this work also provides information for a direct comparison with other systems such as jets with swirl [4].

The superior spreading characteristics of flow issuing from rectangular slots [5], underlies the importance of preferring these over other types of orifice shapes. The flow from rectangular slots has been studied extensively in the past [6–16]. In addition, experiments have been performed using rectangular slots with shaping in planes perpendicular to the mean flow direction [17–19]. From these studies, the centreline mean velocity decay can be separated into three regions, or, perhaps four [11]: the potential core, the typical or characteristic decay region, the transition region and the axisymmetric decay region. The region that appears to have received the most attention is the typical or characteristic decay region for it is here that there are located saddle-backed velocity profiles in the

plane or major axis of the rectangular jet. The saddle-backed velocity profiles seem to be present only when the jet issues from a sharp-edged slot [8, 13]. Moreover, they are not observed when the slot has an aspect ratio of 3 or less; they are not found in square jets for example, duPlessis *et al.* [20], Tsuchiya *et al.* [13] and Schwab [21]. As yet, there is no clear explanation for the occurrence of the saddle-backed velocity profile.

The flow fields of these jets have been mapped by Krothapalli *et al.* [19], Quinn *et al.* [11], Tsuchiya *et al.* [13] and Schwab [21]. These data indicate that the axial velocity decays as $X^{-1.11}$ in the far field, the mean velocities reach self similar behaviour about 30 slot widths downstream of the orifice, the turbulence quantities (i.e. turbulent kinetic energy, Reynolds stresses) do not show self-preserving behaviour for at least 100 slot widths, and that within the characteristic decay region, the fluctuation components of velocity and Reynolds shear stress exhibit significant depressions that are, according to refs. [11, 21], indications of negative production (see for example Hinze [22]).

Studies of the dispersion or distribution of contaminants within jets issuing from three-dimensional slots are limited to those of van der Hegge Zijnen [23], Sfeir [24], Sforza and Stasi [25] and Tsuchiya *et al.* [13]. In all cases, the mean contaminant (either mass or temperature) spread rate or half-width is larger than that for the mean velocity. Moreover, the centreline axial mean temperature decay follows the axial mean velocity decay rate, and for the sharp-edged orifice cases, the mean temperature profiles exhibit the saddle-backed feature found in the axial mean velocity profiles. To the authors' knowledge, no measurements exist of contaminant fluctuation in the literature for the case of flow issuing from rectangular slots.

The purpose of this paper is to present results of

NOMENCLATURE

b	transverse concentration half width, point where $\bar{\Gamma} = 1/2\Gamma_c$	γ	concentration fluctuation, $\bar{\Gamma} - \Gamma$
D	equivalent diameter of the rectangular nozzle, $(4hL/\pi)^{1/2}$	Γ	total concentration
D_H	hydraulic diameter, $2Lh/(L+h)$	σ	wrinkle amplitude, standard deviation of the mean jet transverse length.
h	width of the rectangular slot nozzle	Subscripts	
L	length of the rectangular slot nozzle	Γ	concentration property
n	parameter in equation (8)	c	centreline value
r	transverse distance in a jet flow, equation (8)	o	nozzle or jet source value
Sc	Schmidt number	U	velocity property
X	longitudinal coordinate	y	property in the Y -direction
Y	transverse coordinate	z	property in the Z -direction.
Z	transverse coordinate.	Superscripts	
Greek symbols		$\bar{\quad}$	time average value
β	concentration intermittency	$'$	r.m.s. value.

concentration measurements in a three-dimensional jet. A jet issuing from a sharp-edged slot of aspect ratio 10 has been selected. To measure the mean and fluctuation concentration field, marker nephelometry [26] was used. Estimates for intermittency are provided; these estimates are, too, the first of their kind for this flow situation.

EXPERIMENTAL

The experimental nozzle used in this work is the same as that used by Pollard *et al.* who investigated the velocity field of the jet. For the present study of the concentration field of the jet fluid, this nozzle (aspect ratio of 10, 12.7×127 mm), was mounted on the face of a wind tunnel with a 1 m contraction to the nozzle dimension. Note that the present investigation employed the experimental setup used in refs. [4, 27] and represents a totally new system from that used by Pollard *et al.* The nozzle velocity was set at 55 m s^{-1} , corresponding to a nozzle Reynolds number based on the narrow slot dimension, h , of 4.7×10^4 . An appropriate length scale in the near field is h , while further downstream we might employ the diameter of a round jet with equivalent area, $D = (4hL/\pi)^{1/2}$, and $D/h = 3.57$.

The marker nephelometry system used in the present study was similar to the system described in previous work, see ref. [4]; however, in the present investigation computer data acquisition for the fluctuation signal and a digital storage oscilloscope for intermittency measurements were incorporated. The light source was a 75 mW argon ion laser which could be mounted on various types of traverse rigs to permit measurement of the point source concentration at various places in the flow field. The jet fluid was tagged

with a condensed oil smoke generated by rapid evaporation and cooling of a commercially available oil [28]. The fog stream from this smoke generator was fed directly into the intake of the wind tunnel fan. Mean and fluctuation signals were measured simultaneously with a 100 s time average for all readings. Measurements were taken at random positions repeatedly in the flow field so as to ensure reproducibility of the measurements. Traversing accuracy for all measurements in this work was ± 0.25 mm. Centreline measurements of the mean concentration were taken with the nozzle value as a reference signal for the light-scatter tests while the corresponding centreline value was used for transverse profiles.

Measurements of intermittency were made. Data were recorded on a digital storage oscilloscope (14-bit resolution). These data were stored on floppy disks and processed on a microcomputer to obtain the fraction of time turbulent jet fluid was observed for each point of interest. A total of 2×10^5 points were typically processed for each measurement of intermittency. Typical values of intermittency were in the range of 0.15 and 0.95.

PRESENTATION OF RESULTS

The mean and fluctuation field of the nozzle fluid were measured along the centreline of the flow in the range $0 \leq X/D \leq 60$. The mean centreline concentration decay, $\bar{\Gamma}_c$, relative to the nozzle value, Γ_o , was described by the relations, Fig. 1

$$2.5 \leq X/h \leq 15: \left(\frac{\bar{\Gamma}_c}{\Gamma_o}\right)^2 = 0.348 \left(\frac{X}{h} + 3.59\right)$$

or

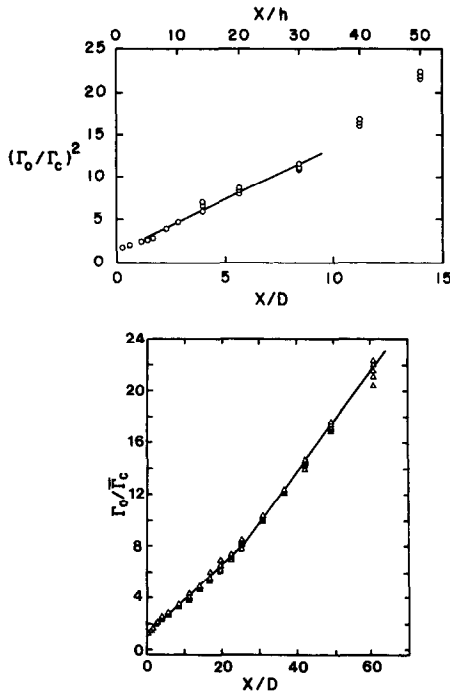


FIG. 1. Centreline mean concentration; nozzle region (top graph) and full region examined in this work.

$$1.4 \leq X/D \leq 8.4: \left(\frac{\Gamma_o}{\Gamma_c}\right)^2 = 1.24 \left(\frac{X}{D} + 1.01\right) \quad (1)$$

$$8 \leq X/D \leq 25: \frac{\Gamma_o}{\Gamma_c} = 0.267 \left(\frac{X}{D} + 4.87\right) \quad (2)$$

$$X/D \geq 25: \frac{\Gamma_o}{\Gamma_c} = 0.382 \left(\frac{X}{D} - 3.74\right) \quad (3)$$

The centreline concentration fluctuation intensity, $\gamma'_c/\bar{\Gamma}_c$, where $\gamma' = (\overline{y^2})^{1/2}$, represents the r.m.s. value of the fluctuation signal, is shown in Fig. 2. Using the approach of Becker *et al.* [3], those data for $\Gamma_o/\bar{\Gamma}_c \geq 2$ can be recast in the form

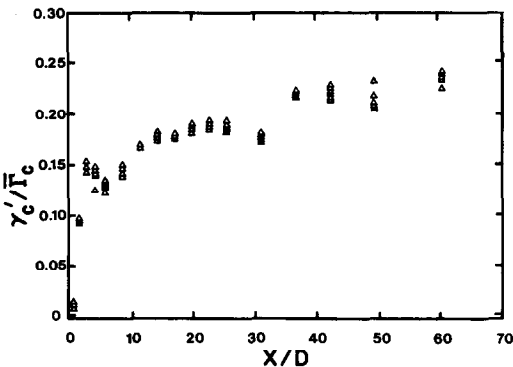


FIG. 2. Centreline fluctuation intensity as a function of downstream position.

$$\frac{\gamma'_c}{\bar{\Gamma}_c} = 0.253 \left/ \left[1 + 2.45 \left(\frac{\bar{\Gamma}_c}{\Gamma_o}\right) \right] \right. \quad (4)$$

while those data further downstream, $\Gamma_o/\bar{\Gamma}_c \geq 12$, can be expressed in the form

$$\frac{\gamma'_c}{\bar{\Gamma}_c} = 0.257 \left/ \left[1 + 2.52 \left(\frac{\bar{\Gamma}_c}{\Gamma_o}\right) \right] \right. \quad (5)$$

indicating that $\gamma'_c/\bar{\Gamma}_c \approx 0.25$ far downstream.

Transverse profiles of the mean concentration field were measured at $X/D = 0.56, 1.40, 2.80, 5.60, 8.40, 11.2, 14.0, 19.6, 25.2, 30.8, 36.4$ and 42.0 . These are equivalent to those locations used previously for the velocity field [11]. The half concentration widths as a function of downstream position are shown in Fig. 3 and can be described by the relations

$$X/D \geq 2.8: \frac{b_z}{D} = 0.130 \left(\frac{X}{D} + 0.54\right) \quad (6)$$

$$X/D \geq 14: \frac{b_y}{D} = 0.152 \left(\frac{X}{D} - 5.0\right) \quad (7)$$

All transverse profiles in this work were obtained by taking measurements totally across the flow using a mean concentration reference position near the centreline and 'folding' the data about the half concentration width for each traverse. Data are presented with the same symbol but with 'open' or 'closed' shading to denote data on opposite sides of the jet centreline.

In the nozzle region, $0 \leq X/D \leq 4$, the mean concentration profiles demonstrate a saddle-back behaviour in the Y -plane, as shown in Fig. 4. The corresponding fluctuation intensity data are also shown in this figure. Transverse profiles of the mean concentration decay in jets with and without swirl typically follow the Gaussian (normal) probability density function [27]

$$\frac{\bar{\Gamma}}{\bar{\Gamma}_c} = e^{-0.693(r/b)^2} \quad (8)$$

where r/b is a transverse position normalized with

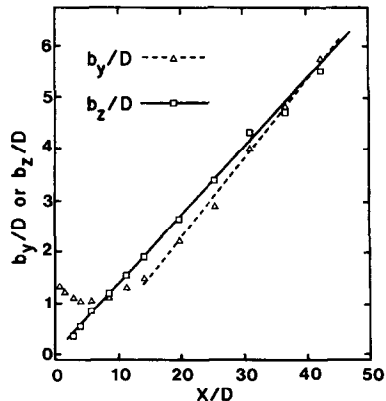


FIG. 3. The half concentration width as a function of downstream position.

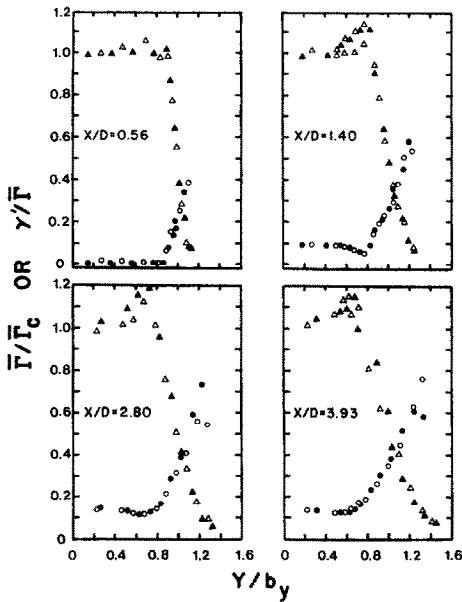


FIG. 4. Transverse mean concentration (triangles) and fluctuation intensity (circles) in the *Y*-plane in the nozzle region. Open and closed shading of the symbols indicate opposite sides of the jet flow.

respect to the jet half concentration scale and $n = 2$. Transverse profiles of the mean concentration field in the *Z*- and *Y*-planes are shown in Figs. 5 and 6 with a separate symbol for each downstream location. In each graph the transverse position is normalized with respect to the half concentration distance appropriate for that plane and downstream position. Those data for $2.8 \leq X/D \leq 14.0$ in the *Z*-plane, Fig. 5, show good symmetry and can be described by the relation

$$\frac{\bar{\Gamma}}{\bar{\Gamma}_c} = e^{-0.693(Z/b_z)^{1.93}} \quad (9)$$

which is in good agreement with equation (8). Those data for $X/D \geq 19.6$ do not indicate as good symmetry and these data can be described by the relations

$$\text{open symbols: } \frac{\bar{\Gamma}}{\bar{\Gamma}_c} = e^{-0.693(Z/b_z)^{1.60}} \quad (10)$$

$$\text{closed symbols: } \frac{\bar{\Gamma}}{\bar{\Gamma}_c} = e^{-0.693(Z/b_z)^{2.39}} \quad (11)$$

Those data in the *Y*-plane, Fig. 6, for $8.4 \leq X/D \leq 14.0$ also indicate good symmetry and can be described by the relation

$$\frac{\bar{\Gamma}}{\bar{\Gamma}_c} = e^{-0.693(Y/b_y)^{2.03}} \quad (12)$$

while those data further downstream, $19.6 \leq X/D \leq 42.0$, also demonstrate a somewhat unsymmetrical behaviour

$$\text{open symbols: } \frac{\bar{\Gamma}}{\bar{\Gamma}_c} = e^{-0.693(Y/b_y)^{1.38}} \quad (13)$$

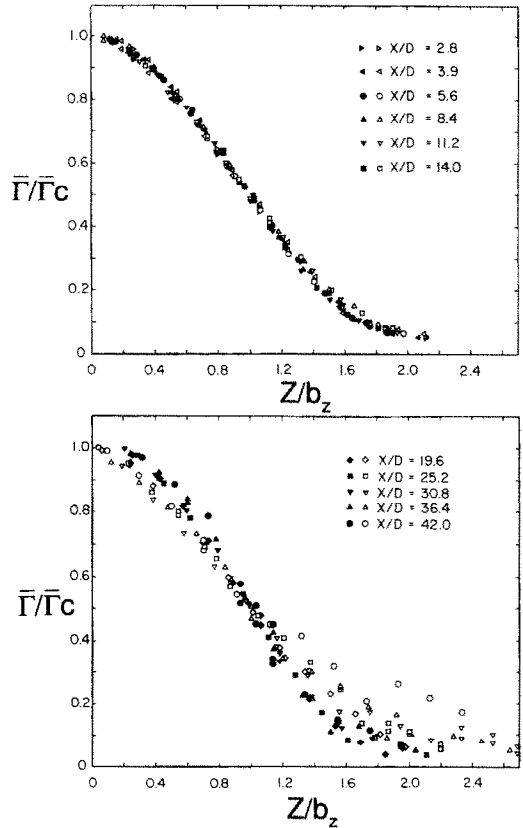


FIG. 5. Transverse mean concentration decay in the *Z*-plane. Open and closed symbols indicate opposite sides of the jet flow.

$$\text{closed symbols: } \frac{\bar{\Gamma}}{\bar{\Gamma}_c} = e^{-0.693(Y/b_y)^{2.40}} \quad (14)$$

Transverse profiles of the concentration fluctuation intensity were also made at the downstream locations noted above and these results are presented in normalized form, γ'/γ'_c , as shown in Fig. 7. Those data in the *Z*-plane for $2.8 \leq X/D \leq 14.0$ indicate good symmetry and some tendency towards a self-similar behaviour; however, those data for $X/D \geq 19.6$ indicate a departure from such a form in that these data appear to display a preferential grouping on either side of the jet as indicated by the open and closed symbols. A similar trend was also noted in the *Y*-plane where some tendency to a self-similar behaviour can be inferred for $8.4 \leq X/D \leq 14.0$ with a deviation from this trend for $X/D \geq 19.6$. The transverse fluctuation intensity can also be related to the mean concentration by the form suggested by Becker *et al.* [3] as shown in Fig. 8. The linear region, typically where $\bar{\Gamma}/\bar{\Gamma}_c \geq 0.3$, can be expressed in the form

$$\text{Z-plane: } \overline{\gamma'^2} = -0.086\bar{\Gamma}^2 + 0.115\bar{\Gamma}\bar{\Gamma}_c \quad (15)$$

$$\text{Y-plane: } \overline{\gamma'^2} = -0.077\bar{\Gamma}^2 + 0.116\bar{\Gamma}\bar{\Gamma}_c \quad (16)$$

and within the experimental error associated with

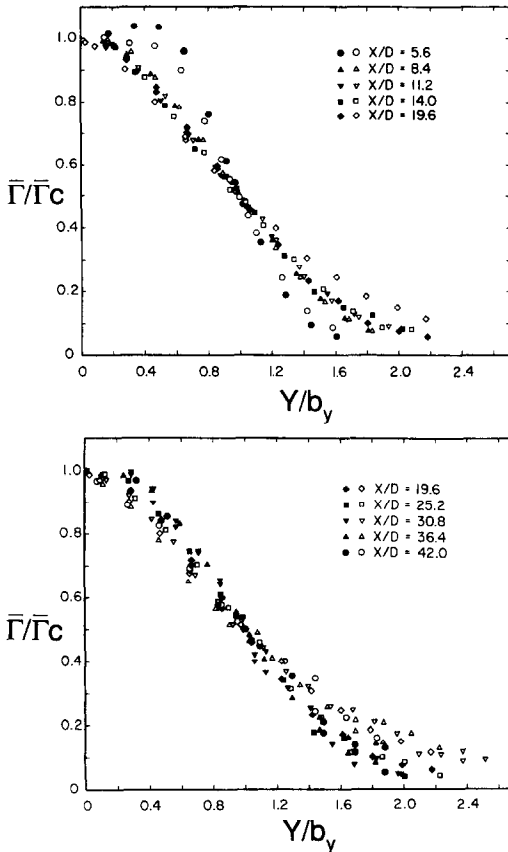


FIG. 6. Transverse mean concentration decay in the Y -plane. Open and closed symbols indicate opposite sides of the jet flow.

these results the data for both planes can be described by

$$\overline{\gamma^2} = -0.083\overline{\Gamma^2} + 0.116\overline{\Gamma}\overline{\Gamma}_c \quad (17)$$

Intermittency measurements were obtained at the same downstream positions as noted for the mean and fluctuation concentration fields. These data, Fig. 9, are presented with the transverse position normalized with respect to the half concentration width at each downstream position as the independent variable. Becker *et al.* [29] suggested the mean position of the jet boundary, or mean jet radius, as the point where the intermittency, $\beta (= \frac{1}{2} \operatorname{erfc}((Z - \bar{Z})/\sqrt{2}\sigma))$ is equal to 0.5 and the width of the intermittent zone, σ , is given by the r.m.s. excursions from the mean jet radius (also termed the 'wrinkle amplitude'). As an example, the wrinkle amplitude for the Z -plane is

$$\sigma = \left[- \int (Z - \bar{Z})^2 \left(\frac{\partial \beta}{\partial Z} \right) d(Z - \bar{Z}) \right]^{1/2} \quad (18)$$

where $Z = \bar{Z}$ when $\beta = 0.5$.

Becker *et al.* [3] showed that the mean and fluctuation concentration fields of the jet fluid are related to the intermittency through the relations

$$\frac{\gamma'_i}{\overline{\Gamma}_i} = \left(\beta \frac{\overline{\gamma^2}}{\overline{\Gamma^2}} - (1 - \beta) \right)^{1/2} \quad (19)$$

where $\overline{\Gamma}_i = \overline{\Gamma}/\beta$.

From Fig. 9, it is clear that in the far field, $X/D \geq 19.6$, there is a departure from symmetry in the Z -plane, while those data for the Y -plane display good symmetry. The mean jet width and the 'wrinkle amplitude' in the Y - and Z -planes as shown in Fig. 10 can be described by

$$\bar{Y} \approx 0.230X \quad (20)$$

$$\sigma_y \approx 0.047X \quad (21)$$

$$\text{open symbols: } \bar{Z} \approx 0.316X \quad (22)$$

$$\sigma_z \approx 0.12X \quad (23)$$

$$\text{closed symbols: } \bar{Z} \approx 0.165X \quad (24)$$

$$\sigma_z \approx 0.044X \quad (25)$$

DISCUSSION OF RESULTS

The present data for the mean and fluctuation scalar field confirms the presence of a saddle-back behaviour in the Y -plane in the near field, a high entrainment rate and some interesting features in the far field of the flow. The experimental techniques used in this work are well established in our laboratories and previous studies have been carried out with the same wind tunnel facility for investigations of jets with and without swirl [4, 27] on a flow scale similar to the present work. The limitations of the marker nephelometry technique have been well documented [26]. For the present studies, the main limitation involves measurement of the mean concentration field far downstream where the oil smoke tracer was transported at velocities of the order of 5 m s^{-1} . In such regions the smoke particle diameter can change due to evaporation and coagulation. The latter effect is small with the smoke concentration employed in the present work but the transit time of smoke particles in the flow must be less than about 0.1 s for particle evaporation to be negligible. Hence measurements in the present system were not extended beyond $X/D \geq 60$ or 2.7 m. Appropriate corrections for the concentration fluctuation signals were employed in this work. These measurements are a 'local' value and depend on the adequacy of the smoke marker to follow the turbulent fluctuations at the point of interest. In the present system, this marker consisted of particles with a diameter of the order of $1 \mu\text{m}$ and only coagulation effects would have an adverse effect on the frequency response of the signal—as noted above this effect would be small in the present work.

Repeat measurements were made for all scalar properties in this study. For centreline measurements of $\overline{\Gamma}$ and γ , the experimental error typically increases with downstream position as demonstrated by the scatter shown in Figs. 1 and 2. In the case of transverse profiles, the 'local' error for estimates of $\overline{\Gamma}/\overline{\Gamma}_c$, γ/γ'_c ,

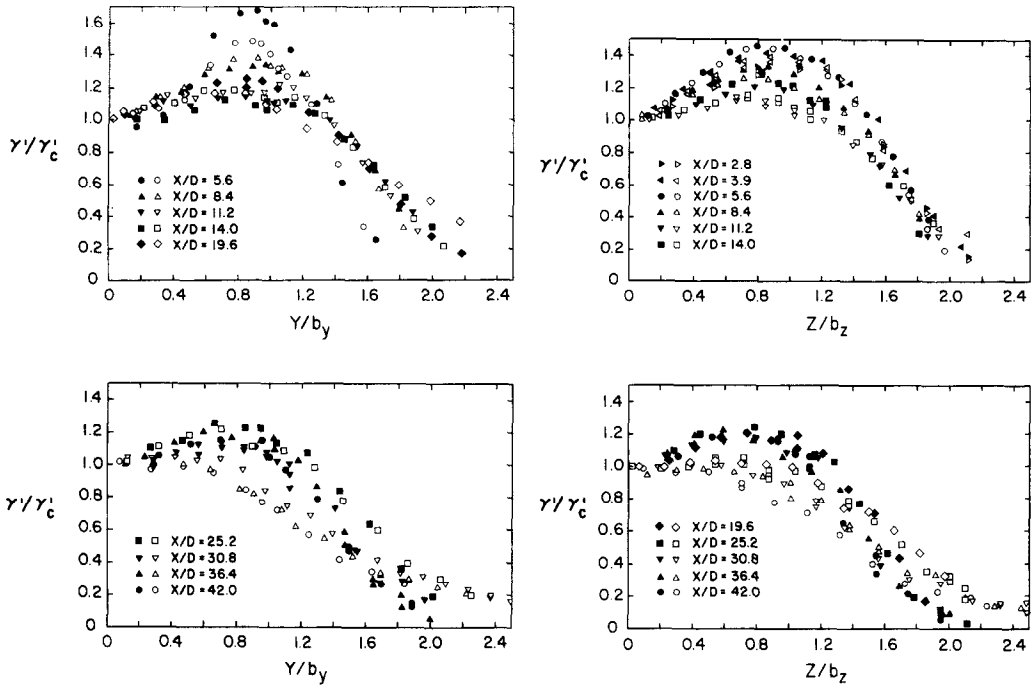


Fig. 7. Transverse concentration fluctuation in the Y - and Z -planes. Open and closed symbols indicate opposite sides of the jet flow.

and β are approximately constant with a pooled standard deviation of 0.015, 0.020 and 0.024, respectively.

The mean concentration decay along the jet centreline in the near field, typically $X/h \leq 30$ ($X/D \leq 8.4$), follows a two-dimensional jet form with $(\Gamma_o/\bar{\Gamma}_c)^2 \approx 0.384(X/h)$. In this region the spreading rate of the jet in the Y -plane, Fig. 3, was relatively constant before increasing at the rate described by equation (7). Further downstream the mean concentration decay displayed two regions of axisymmetric behaviour. For $8 \leq X/D \leq 25$, $\Gamma_o/\bar{\Gamma}_c \approx 0.267(X/D)$ and $\Gamma_o/\bar{\Gamma}_c \approx 0.342(X/D)$ for $X/D \geq 25$. The slower decay law corresponds to the region where the jet spreading rate in the Y -plane tends to the form of equation (7) while the higher decay law appears to correspond to the region where the spreading rate tends to similar values in both planes. The mean concentration decay, equation (3), is about twice that of a round jet where typically $\Gamma_o/\bar{\Gamma}_c \approx 0.185(X/D)$ [3, 27] and more closely simulates the case of a round jet with a swirl level of $S \approx 0.4$ – 0.5 [4]. The nozzle dimension in the present work, $D = (4hL/\pi)^{1/2}$, appears to be a logical choice for this system, however, it is worth noting that if the traditional ‘hydraulic’ diameter, D_H , is chosen we find $D_H = 0.51D$ and $\Gamma_o/\bar{\Gamma}_c \approx 0.196(X/D_H)$, a value quite close to that found for a round jet.

The centreline fluctuation intensity tends to an ultimate value of $\gamma_c/\bar{\Gamma}_c \approx 0.25$, which is slightly higher than that found in round jets with weak or no swirl where $\gamma_c/\bar{\Gamma}_c \approx 0.22$ [4, 27]. Centreline fluctuation intensities of the order of 0.25 have been observed far

downstream in jets with strong swirl [4]. The fluctuation intensity in the present work also exhibits two local minima along the centreline. The first minima occurred near the point where the half concentration widths cross, $X/D \approx 7$, the second as these widths began to coincide near $X/D \approx 30$ and the slope in the centreline mean concentration decay changed from 0.267 to 0.382. These are further illustrated in Fig. 1.

In the nozzle region, the flow exhibited good symmetry in the Y -plane as shown in Fig. 4. The transverse fluctuation intensity remained at a low or minimum value in this region to the point where there occurred the saddle-back in the mean concentration. Transverse profiles of the mean concentration decay exhibited Gaussian type behaviour in the near field region for the Z -plane and for the Y -plane after the effects of the saddle-back behaviour were observed. The half concentration widths in each plane appear to merge in the region $X/D \approx 30$ – 40 and up to that point, the rate of growth was slightly higher in the Y -plane, $b_y \approx 0.15X$, compared with $b_x \approx 0.13X$. Transverse profiles could not be extended beyond $X/D = 42$ in the present work but the form of those data in Fig. 3 would suggest that the jets might continue spreading with similar half concentration widths, $b \approx 0.14X$, in both planes. This is about 30% higher than for a round jet with no swirl where $b \approx 0.105X$ and more comparable to the spreading rates of jets with mild swirl [4]. Flow field results [11, 17, 24], indicate that the velocity half width spreads as $\sim 0.11X$. In addition, it has been reported [11] that the spreading rate in the Y -plane is higher than that of the Z -plane

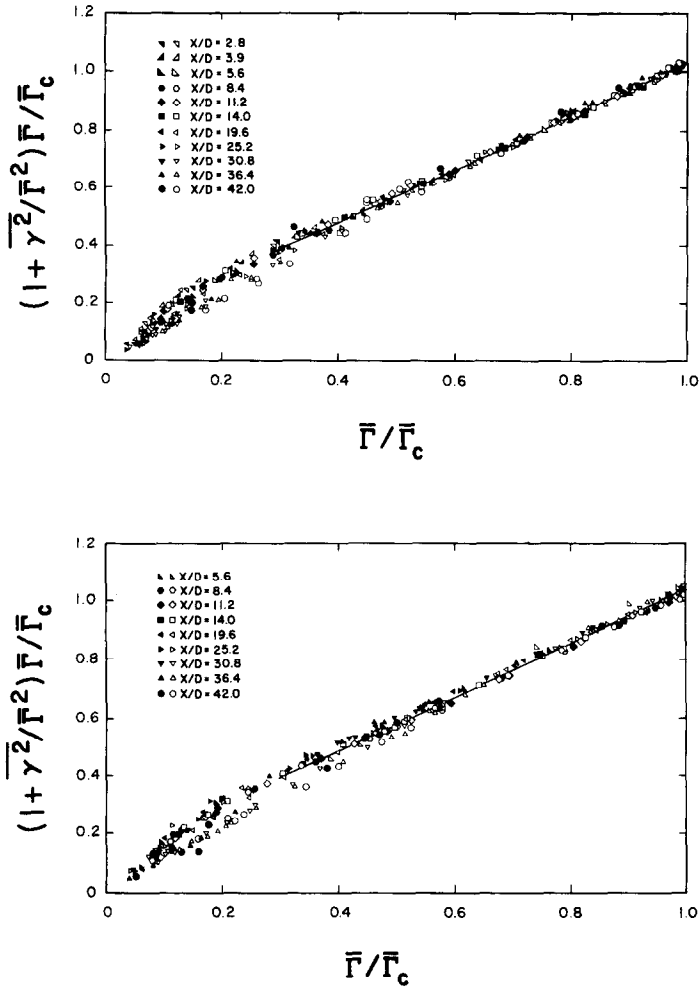


FIG. 8. The relationship between the transverse fluctuation intensity and the mean concentration decay in the Y- (top) and Z-planes (bottom). Open and closed symbols indicate opposite sides of the jet flow.

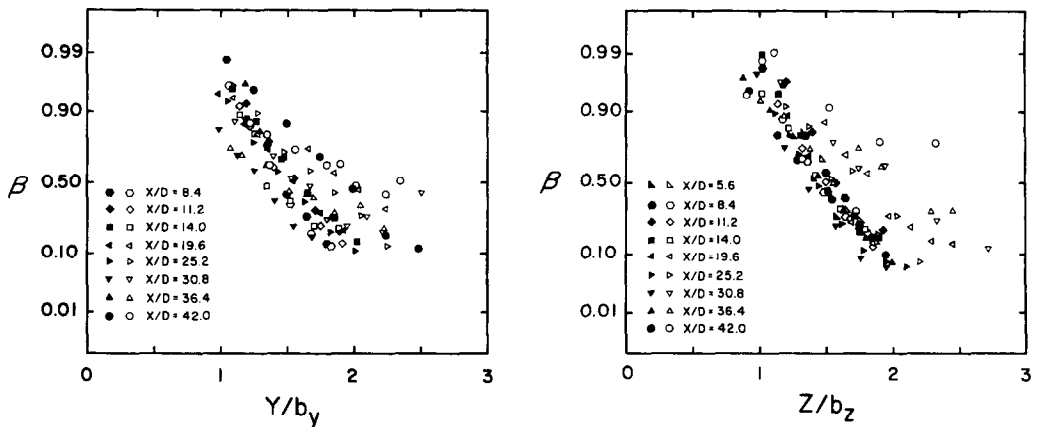


FIG. 9. Transverse concentration intermittency in the Y- and Z-planes. Open and closed symbols indicate opposite sides of the jet flow.

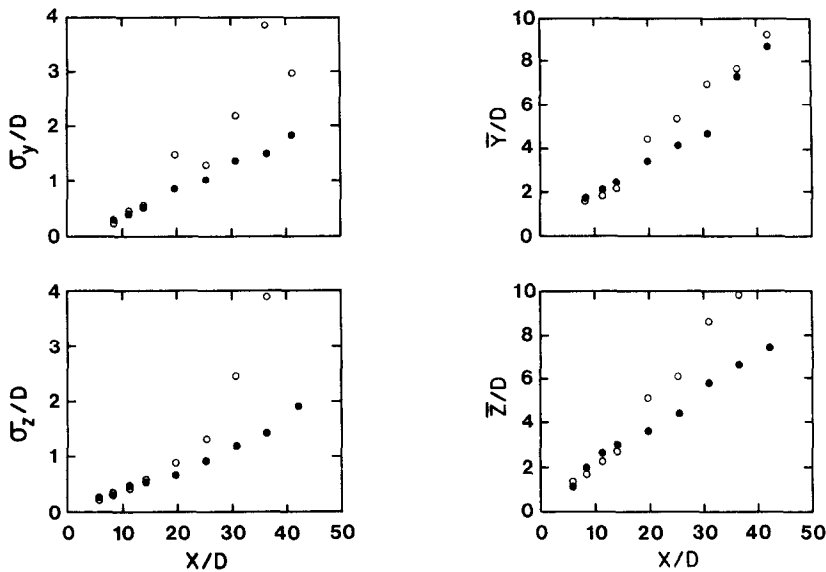


FIG. 10. Mean jet width and wrinkle amplitude in the transverse Y - and Z -planes. Open and closed symbols indicate opposite sides of the jet flow.

for $X/D \leq 50$ as observed in the present study. The present results indicate good symmetry in the near field for both the Y - and Z -planes. However, further downstream, the mean concentration profiles tend to depart from a Gaussian behaviour and a non-symmetrical behaviour was also noted in both planes. This point will be elaborated upon later.

Transverse profiles of the fluctuation intensity also indicated good symmetry in the near field region but a self-similar form of the data was not observed further downstream where a non-symmetrical behaviour was also found in both planes. The fluctuation intensity was adequately described by the form of equation (17), for $\bar{\Gamma}/\Gamma_c \geq 0.3$, demonstrating the utility of this type of correlation.

The present measurements of intermittency provide a very critical test for symmetry in this type of jet flow. In the near field, the data indicated good symmetry for $X/D \leq 14$ but for $X/D \geq 19.6$, the mean jet width, where $\beta = 0.5$, showed distinctly larger values in the Z -plane and the wrinkle amplitude, σ , showed a similar trend in both planes. The data shown in Fig. 9 should be more correctly plotted with the transverse distance normalized with respect to the mean jet width at each downstream location. However, far downstream it is expected that both the half concentration and the mean jet widths should increase linearly with X . The half concentration widths can be more accurately estimated in a flow of this scale and would provide an adequate scaling parameter for the intermittency data. The parameters, b_1 , b_2 , \bar{Y} and \bar{Z} represent transverse scales of the average, inner region of the jet while σ_y and σ_z are representative of the outer, large eddy structure in the flow. The ratios, σ_y/\bar{Y} and σ_z/\bar{Z} , have average values of 0.204 and 0.203, respec-

tively (based on parameters in equations (20)–(25)), compared to values in the range of 0.169–0.212 for jets with no swirl or mild swirl [4]. Close agreement was also observed in the ratios of the parameters, σ_y/b_y and σ_z/b_z , which had average values of 0.309 and 0.338 (equations (6), (7), (21), (23) and (25)), compared with values of 0.309 for jets with no swirl and 0.405 for jets with mild swirl [4]. These results imply that rectangular jets have a large eddy structure similar to round jets with little or no swirl.

Previous work with this type of nozzle in our laboratories has concentrated solely on the mean and fluctuation properties of the velocity field with hot wire anemometry. The width of the mean concentration field, b_Γ , is somewhat larger than the width of the velocity field, b_U , $b_\Gamma/b_U \approx (Sc)^{-1/2}$, where the turbulence Schmidt number, Sc , typically assumes a value of about 0.75, and $b_\Gamma/b_U \approx 1.15$. Alternatively, the half concentration point in a jet flow of this type occurs at the point where the mean velocity is approximately 40% of the centreline value. Hence the present study of the scalar field is quite appropriate for the investigation of flow symmetry.

The first evidence of the non-symmetrical behaviour in this type of jet flow came to light when intermittency measurements were made and the results analysed. A more detailed examination of the transverse mean and fluctuation concentration data suggested that rather than a large amount of scatter, a distinct pattern was indicated. The mean concentration data appear self-similar on different sides of the jet with profiles that start from a Gaussian form closer to the nozzle and then depart from this behaviour further downstream. The transverse concentration fluctuation data reveal a similar trend and

the intermittency data certainly raised doubts about the symmetry of this type of three-dimensional flow for the region examined in this work. Previous measurements of the velocity field have assumed bilateral symmetry for a jet of this type. This work has employed hot wire anemometry and pilot probes as measurement systems with their inherent inaccuracies in regions of high turbulence intensity. The concentration field in the present work has the advantage of providing a wider flow scale with a non-intrusive measurement technique. Hence the results can provide valuable insight regarding the flow symmetry but lacks the detail of the flow structure that might be provided by laser anemometry for example. It should be emphasized that due to limitations of the marker nephelometry technique, the present results of the transverse profiles could only be made to $X/D = 42$. While the transition to axisymmetric behaviour is clearly indicated by these data, additional information would also be required to assess ultimate values of the flow scales and symmetry beyond this region.

CONCLUSION

The scalar concentration field of a sharp-edged rectangular jet with an aspect ratio of 10 has been investigated using marker nephelometry. Measurements include the mean and fluctuation concentration field of the jet fluid and intermittency in both transverse planes for $X/D \leq 42$ with centreline measurements extending to $X/D = 60$. The principle findings of this work are:

(1) In the near field region the flow is characterized by a saddle-back profile in the Y -plane similar to previous findings of the velocity field [8, 11–14], and a half power law decay of the centreline mean concentration for $X/h \leq 30$.

(2) Further downstream the spreading rate of the rectangular jet is about 30% higher than a round jet emanating from a nozzle of the same area. In both transverse planes the mean concentration changes from a Gaussian type distribution to a form that is non-Gaussian and unsymmetrical in both transverse planes. A similar trend for the symmetry is observed for the concentration fluctuation intensity and intermittency data. The mean concentration decay, expressed in terms of the downstream location normalized with respect to the diameter of an equivalent round jet, is described by an axisymmetric jet form with a decay rate about twice that of a round jet.

Acknowledgement—This work was supported by grants from the Natural Sciences and Engineering Research Council of Canada.

REFERENCES

1. F. P. Ricoh and D. B. Spalding, Measurements of entrainment by axisymmetrical turbulent jets, *J. Fluid Mech.* **11**, 21–32 (1961).
2. H. A. Becker and B. D. Booth, Mixing in the interaction zone of two free jets, *A.I.Ch.E. JI* **21**, 949–958 (1975).
3. H. A. Becker, H. C. Hottel and G. C. Williams, The nozzle fluid concentration field of the round, turbulent, free jet, *J. Fluid Mech.* **30**, 285–303 (1967).
4. E. W. Grandmaison and H. A. Becker, Turbulent mixing in free swirling jets, *Can. J. Chem. Engng* **60**, 76–82 (1982).
5. E. W. Grandmaison, S. Ng, A. Pollard and N. L. Zettler, Turbulent mixing in a rectangular jet, 35th Can. Chem. Engng Conf., Calgary, Alberta, Canada (1985).
6. B. G. van der Hegge Zijnen, Measurements of the velocity distribution in a plane turbulent jet, *Appl. Scient. Res.* **1**, 257–276 (1958).
7. A. A. Sfeir, Investigation of three-dimensional turbulent rectangular jets, *AIAA J.* **17**, 1055–1060 (1979).
8. G. F. Marsters, The effects of upstream shaping on incompressible turbulent flows from rectangular nozzles, *Trans. CSME* **5**(4), 197–203 (1978/79).
9. G. F. Marsters, Spanwise velocity distributions in jets with rectangular slots, *AIAA J.* **19**, 148–152 (1981).
10. G. F. Marsters and J. Fotheringham, The influence of aspect ratio on incompressible turbulent flows from rectangular slots, *Aeronaut. Q.* **31**, 285–305 (1980).
11. W. R. Quinn, A. Pollard and G. F. Marsters, Measurements in a turbulent rectangular free jet, 4th Symp. on Turbulent Shear Flows, pp. 7.1–7.6 (1983).
12. W. R. Quinn, A. Pollard and G. F. Marsters, Mean velocity and static pressure distribution in a three dimensional free jet, *AIAA J.* **23**, 971–973 (1985).
13. Y. Tsuchiya, C. Horikoshi and T. Sato, On the spread of rectangular jets, 9th Biennial Symp. on Turbulence, University of Missouri, Rolla, pp. 15.1–15.8 (1984).
14. A. Pollard and M. A. Iwaniw, Flow from sharp-edged rectangular orifices, the effect of corner rounding, *AIAA J.* **23**, 631–633 (1985).
15. R. R. Schwab and A. Pollard, On saddle-backed velocity profiles in three-dimensional free jets, *Proc. Can. Congress of Applied Mechanics*, London, Ontario, Canada, pp. B55–B56 (1985).
16. A. Pollard, R. R. Schwab and E. W. Grandmaison, The three dimensional wall jet—a flow visualization study, 4th Int. Symp. on Flow Visualization, Paris, pp. 523–526 (1986).
17. P. M. Sforza, M. H. Steiger and N. Trentacoste, Studies on three-dimensional viscous jets, *AIAA J.* **4**, 800–806 (1966).
18. N. Trentacoste and P. M. Sforza, Further experimental results for three-dimensional free jets, *AIAA J.* **5**, 885–891 (1967).
19. A. Krothapalli, D. Baganoff and K. Karamcheti, On mixing of a rectangular jet, *J. Fluid Mech.* **107**, 201–220 (1981).
20. M. P. duPlessis, R. L. Wang and R. Kahawita, Investigations of the near field region of a square jet, *Trans. ASME J. Fluids Engng* **96**, 246–251 (1974).
21. R. R. Schwab, An experimental and numerical investigation of three-dimensional jet flows from sharp-edged orifices, Ph.D. Thesis, Department of Mechanical Engineering, Queen's University, Kingston, Ontario, Canada (1986).
22. J. O. Hinze, Turbulent flow regions with shear stress and mean velocity gradient of opposite sign, *Appl. Scient. Res.* **22**, 163–175 (1970).
23. B. G. van der Hegge Zijnen, Measurements of the distribution of heat and matter in a plane turbulent jet of air, *Appl. Scient. Res.* **7**, 277–292 (1958).
24. A. A. Sfeir, The velocity and temperature fields of rectangular jets, *Int. J. Heat Mass Transfer* **19**, 1289–1297 (1976).
25. P. M. Sforza and W. Stasi, Heated three-dimensional turbulent jets, *ASME J. Heat Transfer* **101**, 353–358 (1979).

26. H. A. Becker, Mixing, concentration fluctuations and marker nephelometry. In *Studies in Convection* (Edited by B. E. Launder), Vol. 2, pp. 45–139. Academic Press, London (1977).
27. E. W. Grandmaison, D. E. Rathgeber and H. A. Becker, Some characteristics of concentration fluctuations in free turbulent jets. *Can. J. Chem. Engng* **60**, 212–219 (1982).
28. E. W. Grandmaison, S. Ng and H. A. Becker, A smoke generation system for fluid dynamics research, *J. Phys. Series E: Scient. Instrum.* **20**, 606–608 (1987).
29. H. A. Becker, H. C. Hottell and G. C. Williams, Concentration intermittency in jets, Tenth Symp. (Int.) on Combustion, The Combustion Institute, Pittsburgh, Pennsylvania, pp. 1253–1263 (1965).

MELANGE SCALAIRE DANS UN JET TURBULENT RECTANGULAIRE

Résumé—On étudie à l'aide d'un marquage par néphélogétrie le champ de mélange scalaire d'un jet turbulent sortant d'un orifice rectangulaire à bord mince avec un rapport de forme égal à 10. Les résultats incluent le champ de concentration moyen et instantané et l'intermittance. Dans la région proche, la décroissance de la concentration moyenne est caractérisée par la dimension étroite du jet, le profil caractéristique du champ des vitesses est observé et une bonne symétrie est démontrée pour les propriétés scalaires. Dans la région lointaine de l'écoulement, la décroissance de la concentration moyenne est caractérisée par une échelle de longueur équivalente à un jet circulaire avec la même section d'orifice. Basé sur cette longueur d'échelle la décroissance sur l'axe est environ deux fois celle du jet circulaire. De plus les profils transversaux de concentration moyenne, la concentration fluctuante et l'intermittance montrent un écart à la symétrie dans tous les plans.

MISCHVORGÄNGE IN EINEM FREIEN TURBULENTEN RECHTECKIGEN STRAHL

Zusammenfassung—Das skalare Mischungsfeld eines turbulenten Strahls, der aus einer scharfkantigen rechteckigen Düse mit dem Seitenverhältnis 10 austritt, wird unter Verwendung der Nephelometrie untersucht. Es werden Ergebnisse für den Mittelwert und die Fluktuation der Konzentration im Fluid angegeben. Im Gebiet nahe der Strömung fällt die mittlere Konzentration aufgrund der geringen Abmessung des Strahls ab. Das Geschwindigkeitsfeld zeigt ein sattelförmiges Profil. Die skalaren Eigenschaften weisen eine gute Symmetrie auf. In größerer Entfernung von der Strömung ist der Abfall der Konzentration durch einen Längenmaßstab gekennzeichnet, der demjenigen bei einem runden Strahl und gleichem Düsenquerschnitt äquivalent ist. Auf der Grundlage dieses Längenmaßstabs erweist sich der Konzentrationsabfall entlang der Mittellinie als zweimal so groß wie beim runden Strahl. Darüberhinaus zeigen die Profile der mittleren Konzentration und der Konzentrationsschwankung in beiden Ebenen quer zur Strömung eine Abweichung von der Symmetrie.

СКАЛЯРНОЕ СМЕШЕНИЕ В СВОБОДНОЙ ТУРБУЛЕНТНОЙ ПРЯМОУГОЛЬНОЙ СТРУЕ

Аннотация—С использованием маркерной нефелометрии исследуется скалярное поле смешения турбулентной струи, истекающей из прямоугольного отверстия с острыми краями, отношение сторон которого равно 10. Полученные результаты включают поле средних и флуктуационных концентраций для истекающей из сопла жидкости, а также перемежаемость. В ближней области течения уменьшение средней концентрации определяется меньшей стороной сечения, наблюдается седлообразный профиль поля скорости, а скалярные свойства обнаруживают хорошую симметрию. В дальней области течения уменьшение средней концентрации характеризуется масштабом длины, эквивалентным круглой струе с той же площадью отверстия. На основе упомянутого масштаба длины уменьшение осевой средней концентрации почти вдвое больше по сравнению со случаем круглой струи. Кроме того, поперечные профили средней и флуктуационной концентрации, а также перемежаемость указывают на отклонение от симметрии в обеих плоскостях.